Supporting information for

Hyper-electronegativity fluorine induced electron localization enables highly efficient and stable oxygen evolution electrocatalysis on Vo-rich cobalt-iron oxides

Zirui Wu,[‡, a] Chun Kong,[‡, a] Yongying Wang,[a] Juan Xie,[c] Yi Li,[*, a, b], Juan Yang,[*, a]

[a]School of Materials Science and Engineering, Jiangsu University, Zhenjiang 212013, China

[b]National Laboratory of Solid State Microstructures, School of Physics, Nanjing University, Nanjing 210093, China

[c]School of Textile, Garment and Design, Suzhou University of Technology, Changshu 215500, China

[*]Corresponding author.

Email: liyi5482@ujs.edu.cn; yangjuan6347@ujs.edu.cn

[‡]These authors contributed equally to this work.

Experimental section

1. Chemicals and materials

Cobaltous nitrate hexahydrate [$Co(NO_3)_2·6H_2O$, 99%], iron nitrate nonahydrate [$Fe(NO_3)_3·9H_2O$, 99%)], urea [$CO(NH_2)_2$, 99%] and ammonium fluoride (NH_4F, 99.99%) were purchased from Shanghai Aladdin Bio-Chem Technology Co., Ltd. Nickel foam (NF) was purchased from Suzhou Sinero Technology Co., Ltd. Sodium borohydride ($NaBH_4$, 99%) and ethanol (C_2H_6O) was purchased from Sinopharm Chemical Reagent Co., Ltd. The deionized (DI) water used in all experiments was obtained from a Millipore system. All chemicals were used without further purification.

2. Synthesis of CoFe(OH)F/NF

Firstly, a block of NF (2 × 3 cm) was carefully treated with hydrochloric acid (1 M), acetone, and ultra-pure water in an ultrasound bath for 15 min each time. The processed NF was dried in a vacuum oven overnight. For a typical synthesis, 1 mmol (0.291 g) $Co(NO_3)_2·6H_2O$, 0.5 mmol (0.202 g) $Fe(NO_3)_3·9H_2O$, 1.5 mmol (93 mg) NH_4F and 5 mmol (0.3 g) urea were dissolved in 20 mL of DI water under continuous stirring. After 30 min, the transparent solution was transferred in to a 100 mL polytetrafluorethylene reactor with a pretreated NF. The reactor was heated at 120 °C for 6 h. The product was washed with DI water several times and vacuum-dried overnight. The product was denoted as CoFe(OH)F/NF. As a comparison, we fabricated a range of samples through a consistent methodology, varying the proportions of Co and Fe precursors as well as adjusting the quantity of NH_4F utilized.

3. Synthesis of F-CoFeO_x/NF

During the pyrolysis process, CoFe(OH)F/NF was employed as the precursor and

subsequently annealed in air at 350 °C for 2 h with a heating rate of 5 °C min^{-1}. The resulting material was denoted as F-$CoFeO_x$@NF.

4. Synthesis of F-$CoFeO_x$-V_O/NF

A 5 mL aqueous solution containing 2 M $NaBH_4$ and 0.1 M NaOH was prepared. The as-obtained F-$CoFeO_x$/NF was immersed in this solution and allowed to react for 10 min. After thorough washing with DI water and drying at 60 °C in a vacuum oven overnight, the final product was obtained and denoted as F-$CoFeO_x$-V_O/NF.

5. Physical characterization

The morphology of the samples was characterized by scanning electron microscope (SEM, JSM-7800 F), at operating voltage of 20 kV. Transmission electron microscopy (TEM) images of samples were obtained using Hitachi, H-7800 operating at an accelerating voltage of 300 kV. High-resolution transmission electron microscopy (HR-TEM, Tecnai, G2-F30) images were recorded on an at operating voltage of 300 kV. The elemental area mapping was analyzed by EDS. The crystalline phases of the catalysts were investigated by employing powder X-ray diffraction (XRD, D8, ADVANCE) on a BRUKER diffractometer with Cu-Kα ($\lambda_{K\alpha1}$=1.5406 Å) radiation sources operated at 40 kV and 30 mA. X-ray photoelectron spectroscopy (XPS) analysis was performed on an ESCALAB 250 X-ray photoelectron spectrometer (Thermo, America) equipped with Al-$K\alpha_{1,2}$ monochromatized radiations at 1,486.6 eV X-ray source. Electron Paramagnetic Resonance (EPR) measurements were run on a Bruker EPRA300 spectrometer at 77 K.

6. Electrochemical measurements

All electrochemical tests were performed in a typical three-electrode electrochemical cell using a CHI760e (Chen Hua, Shanghai) in 1 M KOH. A graphite rod and an Hg/HgO were used as the counter and reference electrodes, respectively. All potentials in this study are given to relative to the reversible hydrogen electrode (RHE) after transformation:

$$E_{RHE} = E_{Hg/HgO} + 0.098 + 0.059pH$$

To evaluated electrochemical performance for different catalysts, the working electrode was put through 20 cyclic voltammetry (CV) scans at 50 mV s^{-1} to clean and stabilize the surface of the catalyst. All linear sweep voltammetry (LSV) polarization curves were obtained with 95% iR-compensation at a scan rate of 5 mV s^{-1} in the O_2-saturated electrolyte. Solution resistance (R_s) was measured by potentiostatic electrochemical impedance spectroscopy (EIS) at frequencies ranging from 0.1 Hz to 100 kHz under open circuit voltage, and the results are presented in the form of a Nyquist plot. The ECSA was determined by:

$$ECSA = \frac{C_{dl}}{C_s}$$

The C_{dl} is double-layer capacitance and C_s is the specific capacitance of the sample. In this study, a general specific capacitance of $C_s = 0.035$ mF cm^{-2} was used based on typical reported values. C_{dl} was determined by the equation $C_{dl} = i_c/v$, where i_c is the charging current and v the scan rate. A series of CV tests in the non-faradaic potential region 1.05–1.15 V (versus RHE) under different scan rates (10, 20, 30, 40, 50 and 60 mV s^{-1}) were performed. And by plotting measured i_c versus ν, C_{dl} was obtained

from the slopes of the linear fitting.

7. Computational details

The spin-unrestricted first-principles method was applied to carry out all the calculations, executed by the Vienna Ab-initio Simulation Package (VASP)[1] with Projector augmented wave (PAW)[2] pseudopotential and GGA-PBE functional.[3] For the optimization of the $CoFeO_x$, F-$CoFeO_x$ and F-$CoFeO_x$-V_O, the bottom two layers were fixed into the bulk position, the other layer and adsorbates were relaxed fully, a gamma point grid and 5 × 5 × 1 *k*-point grid was used for the geometric optimizations and static simulations. The vacuum layer thickness is about 15 Å. The kinetic energy cutoff with the plane wave basis set was 400 eV, and the convergence criteria for the total energy and residual force per atom was less than 10^{-4} eV and 0.02 eV $Å^{-1}$, respectively. Furthermore, the electronic structure simulations were adopted by using density of states and differential charge density calculations by VASPKIT software.[4]

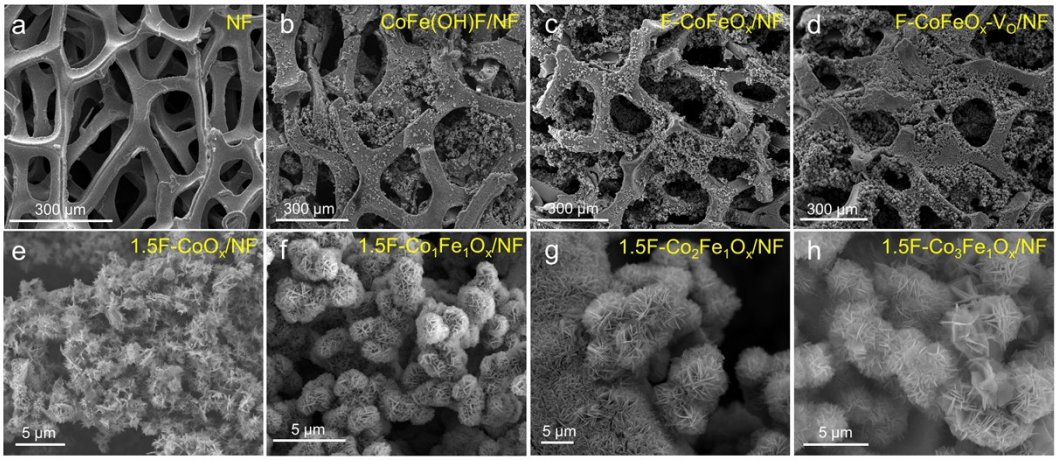

Figure S1. The SEM images of different catalysts.

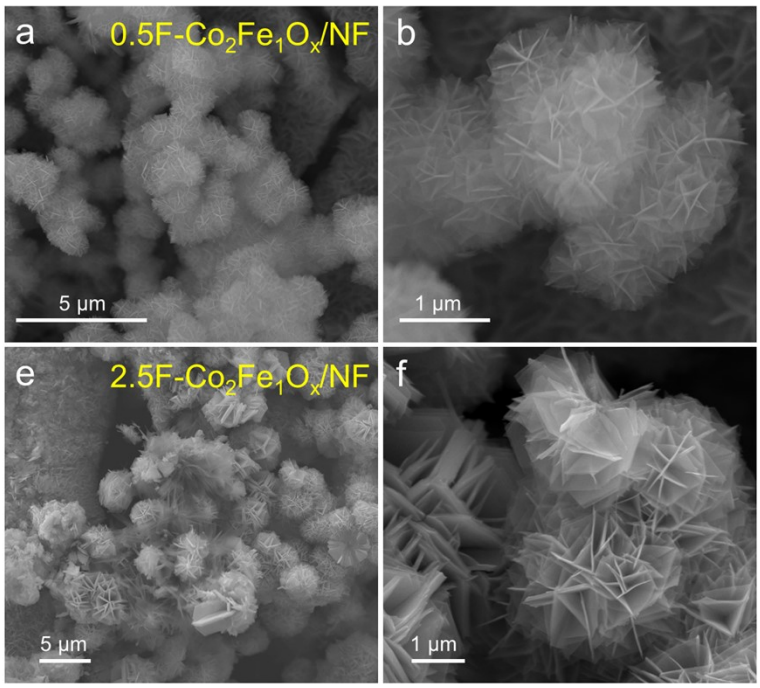

Figure S2. The SEM images of yF-$Co_2Fe_1O_x$/NF. (a, b) 0.5F-$Co_2Fe_1O_x$/NF. (c, d) 2.5F-$Co_2Fe_1O_x$/NF.

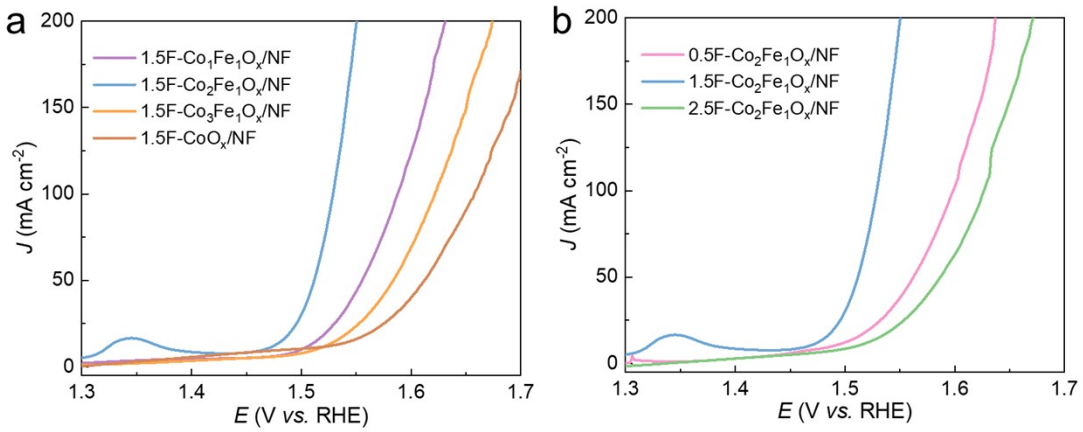

Figure S3. The LSV curves of prepared samples. (a) 1.5F-$Co_mFe_nO_x$/NF. (b) yF-$Co_2Fe_1O_x$/NF.

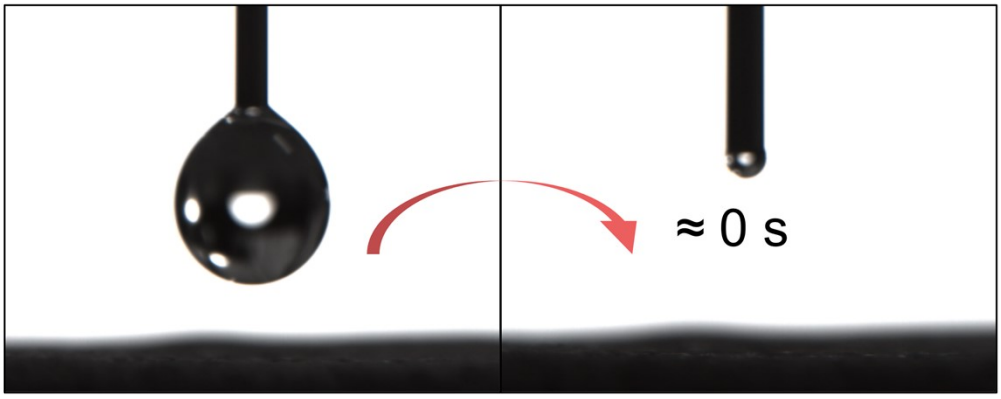

Figure S4. Contact angle photographs of F-$CoFeO_x$-V_O/NF.

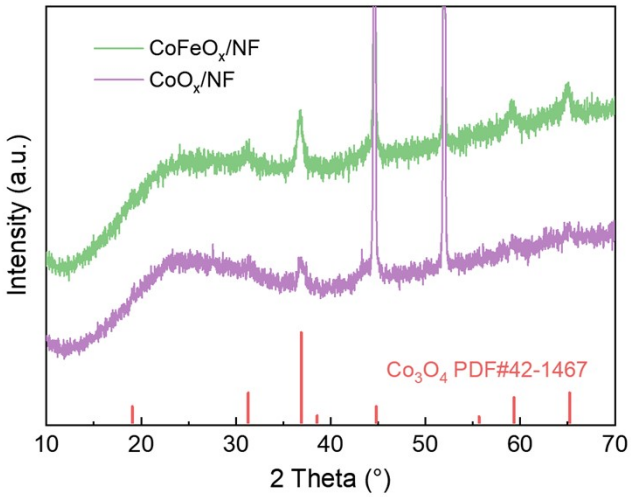

Figure S5. XRD patterns of $CoFeO_x$/NF and CoO_x/NF.

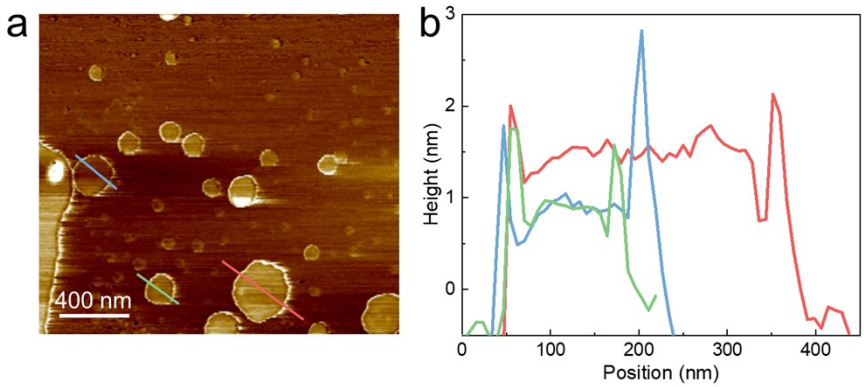

Figure S6. (a) Thickness measurement of F-CoFeO$_x$-V$_O$/NF nanosheets by AFM. (b) The corresponding thickness of F-CoFeO$_x$-V$_O$/NF nanosheets.

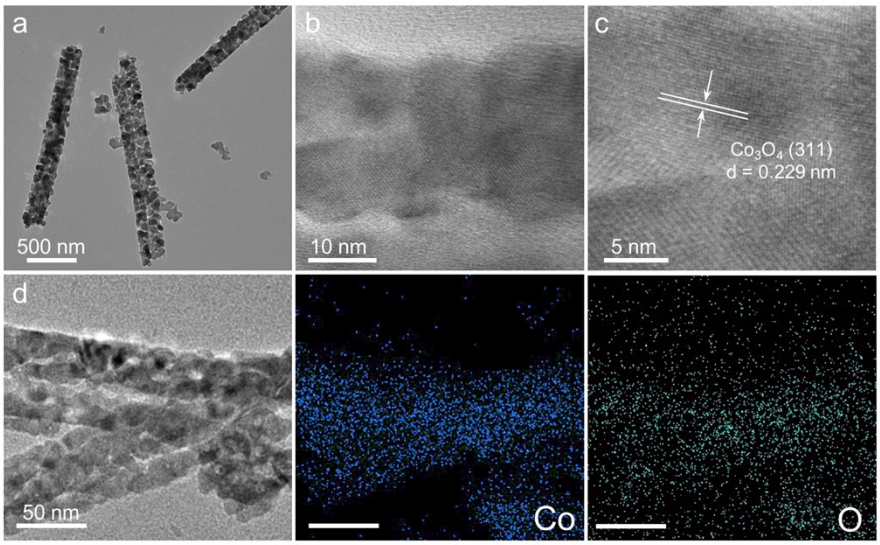

Figure S7. (a) TEM image, (b, c) HR-TEM images, (d) TEM image and he corresponding EDS metal mappings of CoO_x/NF.

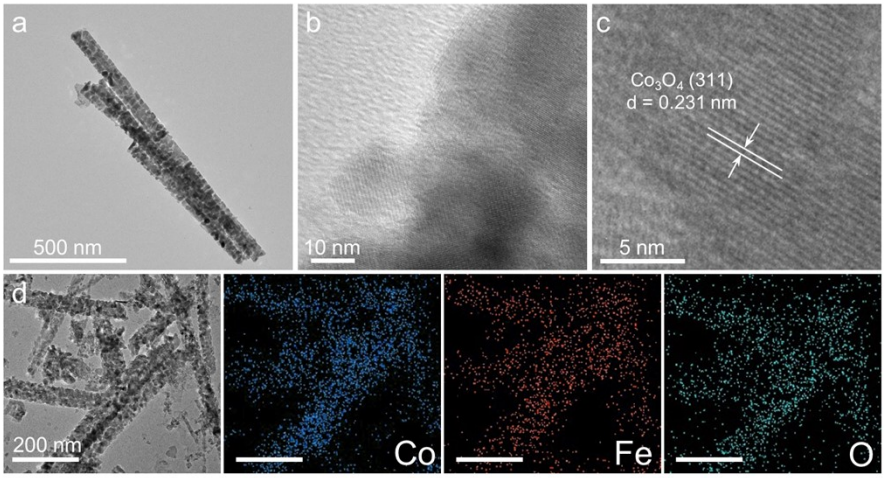

Figure S8. (a) TEM image, (b, c) HR-TEM images, (d) TEM image and he corresponding EDS metal mappings of $CoFeO_x$/NF.

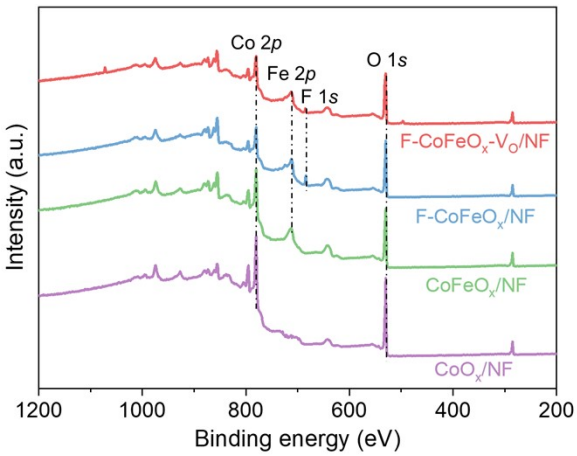

Figure S9. XPS survey spectra for F-CoFeO$_x$-V$_O$/NF, F-CoFeO$_x$/NF, CoFeO$_x$/NF and CoO$_x$/NF.

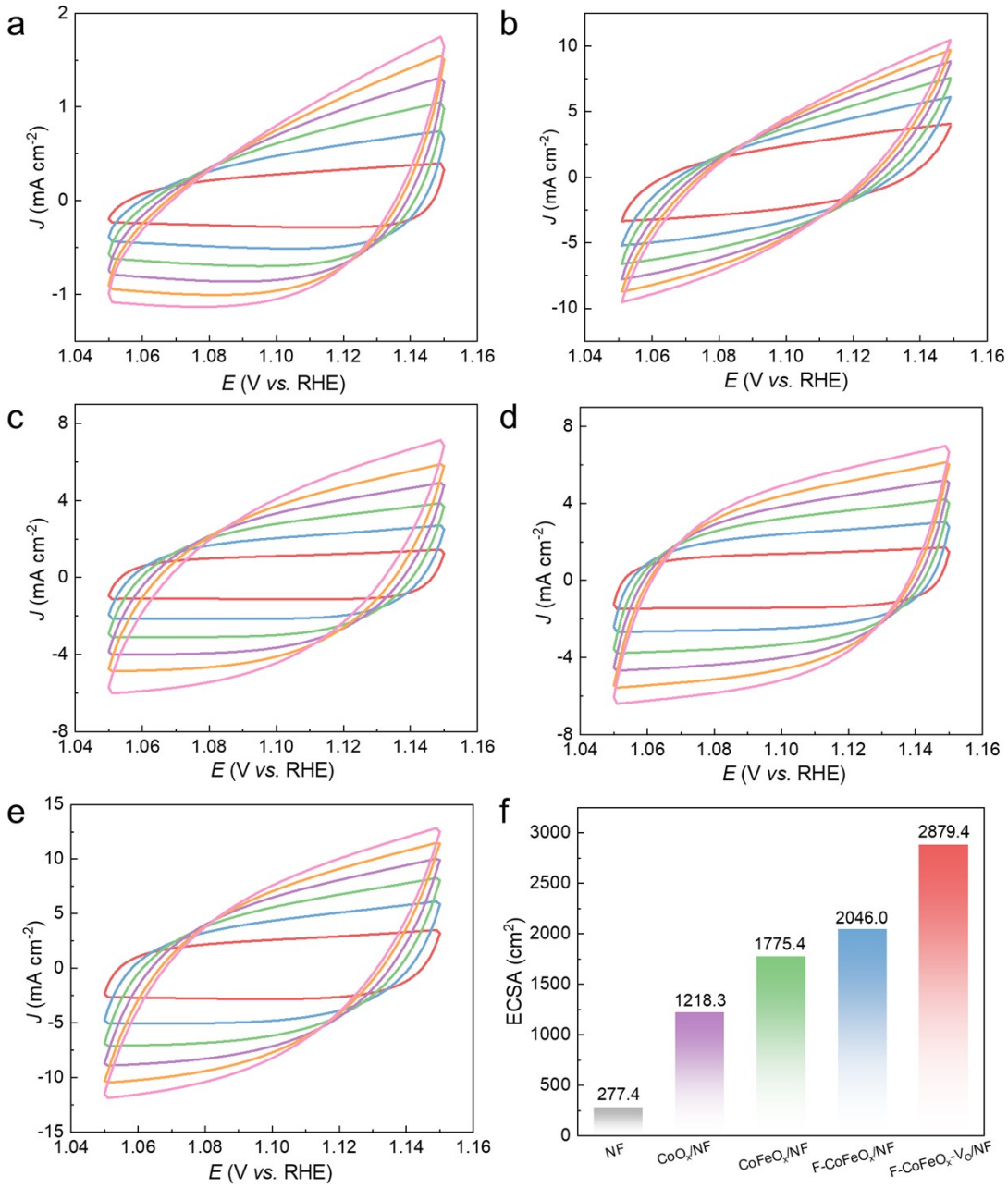

Figure S10. Electrochemically active surface areas analysis. CV curves of (a) NF, (b) CoO_x/NF, (c) $CoFeO_x$/NF, (d) F-$CoFeO_x$/NF, (e) F-$CoFeO_x$-V_O/NF. in the non-Faradaic region in 1 M KOH, obtained at different scanning rates. (f) ECSA values of different samples calculated by C_{dl}.

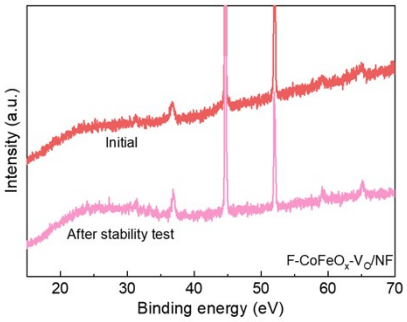

Figure S11. XRD patterns of F-CoFeO$_x$-V$_O$/NF before and after 240 h stability test.

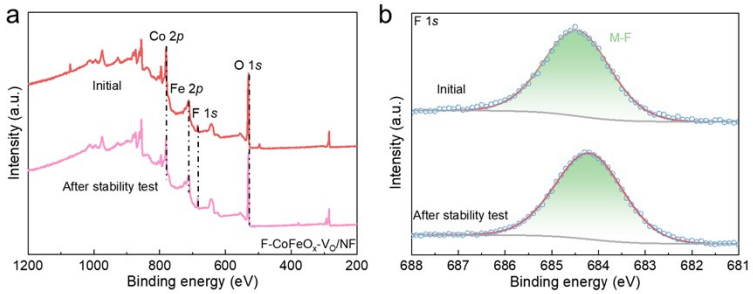

Figure S12. (a) XPS survey spectra, high-resolution XPS spectra of (b) F 1*s* for F-$CoFeO_x$-V_O/NF before and after 240 h stability test.

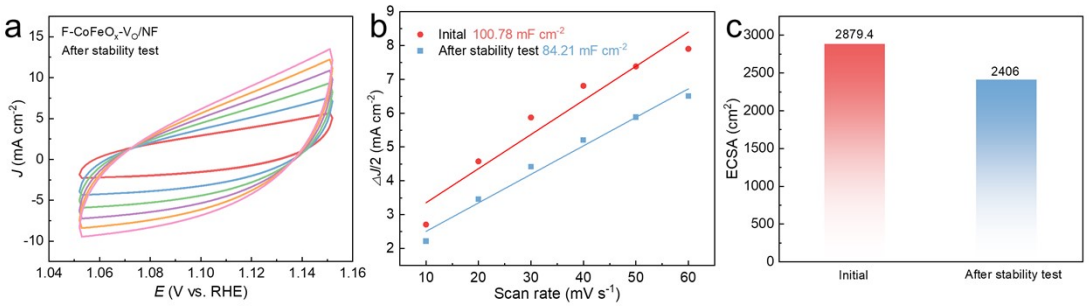

Figure S13. (a) Electrochemically active surface areas analysis. CV curves of F-CoFeO$_x$-V$_O$/NF, (b) C_{dl} plots, (c) ECSA values of different samples calculated by C_{dl}.of F-CoFeO$_x$-V$_O$/NF after 240 h stability test.

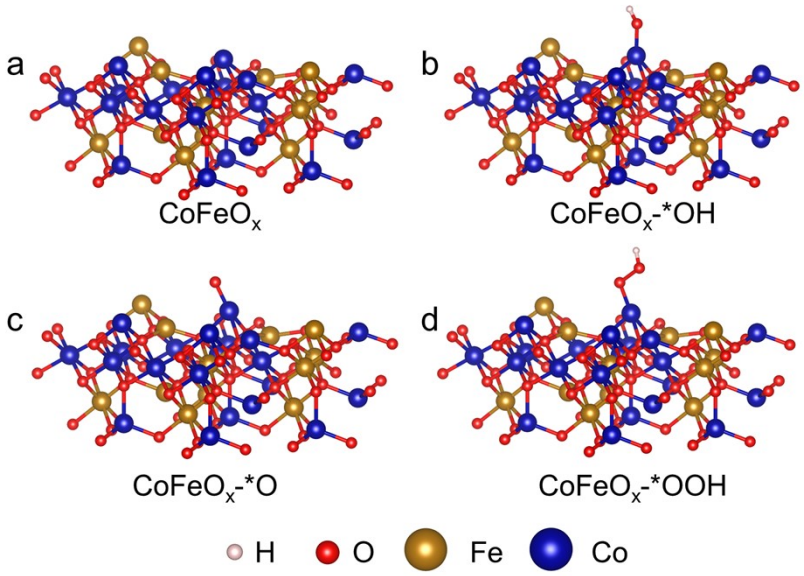

Figure S14. DFT optimized geometries of intermediates for OER on $CoFeO_x$. (a) surface, (b) *O, (c) *OH, (d) *OOH.

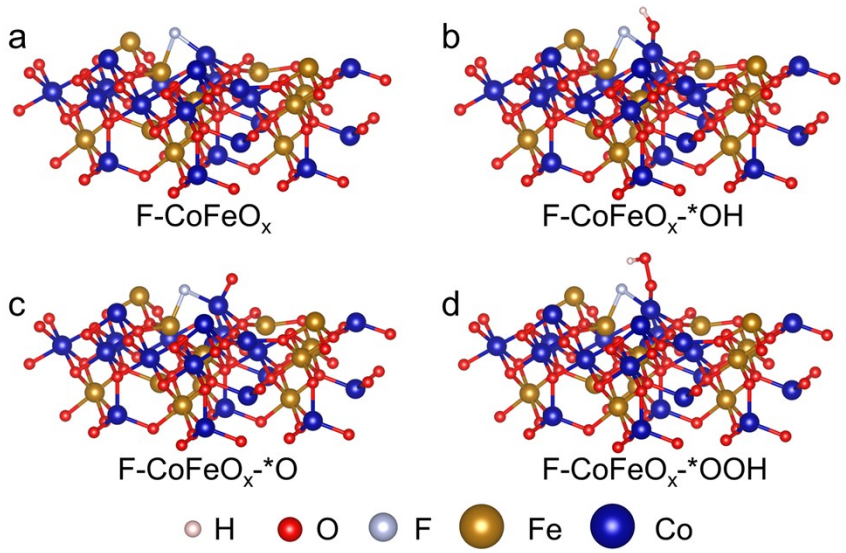

Figure S15. DFT optimized geometries of intermediates for OER on F-CoFeO$_x$. (a) surface, (b) *O, (c) *OH, (d) *OOH.

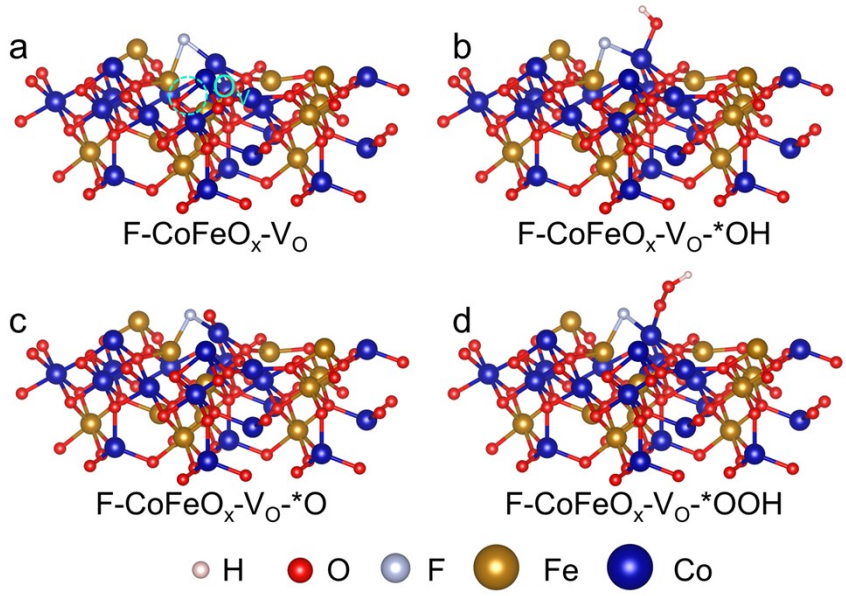

Figure S16. DFT optimized geometries of intermediates for OER on F-CoFeO$_x$-V$_O$. (a) surface, (b) *O, (c) *OH, (d) *OOH.

Table S1. Elemental quantification (at. %) determined by XPS for different samples

Samples	Co (at. %)	Fe (at. %)	O (at. %)	F (at. %)
F-$CoFeO_x$-V_O/NF	14.41	6.51	50.06	2.70
F-$CoFeO_x$/NF	13.37	6.18	52.33	5.93
$CoFeO_x$/NF	14.52	6.26	51.38	/
CoO_x/NF	19.86	/	50.92	/

Table S2. The Co^{2+}/Co^{3+} and Fe^{2+}/Fe^{3+} ratios of different samples. The content of Co^{2+}/Co^{3+} and Fe^{2+}/Fe^{3+} species was determined from the absolute area of each peak obtained through Co 2*p* and Fe 2*p* XPS peaks fitting.

Samples	Co^{2+}/Co^{3+}	Fe^{2+}/Fe^{3+}
F-$CoFeO_x$-V_O/NF	0.98	1.09
F-$CoFeO_x$/NF	1.06	1.18
$CoFeO_x$/NF	0.90	0.76
CoO_x/NF	0.24	/

Table S3. The O_V/O_L ratios of different samples.

Samples	O_V/O_L
F-$CoFeO_x$-V_O/NF	1.15
F-$CoFeO_x$/NF	1.03
$CoFeO_x$/NF	0.76
CoO_x/NF	0.53

Table S4. Comparison of the electrocatalytic performances for OER in alkaline electrolyte.

Catalysts	Overpotential (@10 mA cm^{-2})	Tafel slope (mV dec^{-1})	Durability (h)	References
F-$CoFeO_x$-V_O/NF	**201**	**37.9**	**350 (@100 mA cm^{-2})**	**This work**
$NiCo_2O_4$-F_1	300	96	100 (@100 mA cm^{-2})	5
$FeCoO_x/SiW_{12}O_{40}$	277	44.6	60 (@100 mA cm^{-2})	6
W-Co_3O_4	261	49.8	290 (@10 mA cm^{-2})	7
PO_4^{3-}-$CoFeO_x$	249	29.31	300 (@1.633 V vs. RHE)	8
N,F-Co_3O_4	254	51.5	240 (@20 mA cm^{-2})	9
CoFe/$CoFe_2O_4$@NC	330	126.2	100 (@50 mA cm^{-2})	10
$NiCo_2O_4$	236	40.6	30 (@100 mA cm^{-2})	11
V_O-$CoMoVO_x$	248	72.4	-	12
$ZnCo_2O_{4-x}F_x$/CNTs	350	59.2	13 (@10 mA cm^{-2})	13

Table S5. The parameters of anion exchange membrane.

Producer	Thickness (μm)	Density (mg m^{-2})	Conductivity (mS cm^{-1})	Exchange capacity (meq g^{-1})
FuMA-Tech-3-50	50	6.0–8.5	3–8	1.6–2.1

Table S6. Elemental quantification (at. %) determined by XPS for F-$CoFeO_x$-V_O/NF before and after 240 h CP test.

Samples	Co (at. %)	Fe (at. %)	O (at. %)	F (at. %)
Initial	14.41	6.51	50.06	2.7
After 240 h CP test	14.17	6.23	54.19	2.6

Table S7. The Co^{2+}/Co^{3+}, Fe^{2+}/Fe^{3+} and O_V/O_L ratios for F-$CoFeO_x$-V_O/NF before and after stability test.

	Co^{2+}/Co^{3+}	Fe^{2+}/Fe^{3+}	O_V/O_L
Initial	0.98	1.09	1.15
After stability test	0.92	0.99	1.13

References

1. Y. Li, Z. Cao, Y. Wang, B. Li, J. Yang and Z. Sun, *J. Colloid Interface Sci.*, 2024, **655**, 508–517.
2. P. E. Blöchl, *Phys. Rev. B*, 1994, **50**, 17953−17979.
3. S. Grimme, J. Antony, S. Ehrlich and H. Krieg, *J. Chem. Phys.*, 2010, **132**, 154104.
4. V. Wang, N. Xu, J.-C. Liu, G. Tang and W.-T. Geng, *Comput. Phys. Commun.*, 2021, **267**, 108033.
5. Y. Yue, X. Zhong, M. Sun, J. Du, W. Gao, W. Hu, C. Zhao, J. Li, B. Huang, Z. Li and C. Li, *Adv. Mater.*, 2025, **37**, e2418058.
6. J. Liu, Y. Liu, Y. Wang, L. Zheng, W. He, M. Han, L. Gan, G. I. N. Waterhouse, J. Liu and J. Li, *Small*, 2025, **21**, e12000.
7. Y. Wang, B. Jia, W. Qin, Y. Wang, S. Liu, Y. Qin, Y. Zhao, L. Liu, D. Zhang, H. Liu, H. Zhong, J. Liu, J. Tu, Y. Liu, H. Wu, D. Zhang, J. Fan, X. Qu, H. Li and M. Qin, *J. Am. Chem. Soc.*, 2025, **147**, 32249–32262.
8. X. He, M. Liu, F. Liu, X. Liu, H. Liao, P. Tan and J. Pan, *Adv. Funct. Mater.*, 2025, **35**, e05936.
9. C. Li, B. Ye, B. Ouyang, T. Zhang, T. Tang, Z. Qiu, S. Li, Y. Li, R. Chen, W. Wen, M. Song, B. Mei, X. Xia and Y. Zhang, *Adv. Mater.*, 2025, **37**, e2501381.
10. F.-Y. Guo, J. Luan, X.-C. Meng, P. Zheng, W.-L. Duan and W.-Z. Li, *Chem. Eng. J.*, 2025, **523**.
11. T. Li, W. Shi, J. Meng, Y.-Q. Liu, H. Zhao, Y. Wang and X. Shao, *ACS Catalysis*,

2026, **16**, 4855−4867.

12. N. Luo, A. Cai, J. Pei, X. Zeng, X. Wang and N. Yao, *Adv. Funct. Mater.*, 2025, **35**, 2425503.
13. K. Xiao, Y. Wang, P. Wu, L. Hou and Z. Q. Liu, *Angew. Chem. Int. Ed.*, 2023, **62**, e202301408.